Altimetric Observations of Rossby Wave Variability near Topography

Gary T. Mitchum

Department of Oceanography, University of Hawaii, Honolulu, HI

Abstract. Precise satellite altimetry began with the GEOSAT mission and has reached maturity with the TOPEX/POSEIDON mission. The sea surface height measurements from these instruments are capable of obtaining near-synoptic temporal coverage with a spatial resolution of order 100-300 km and an accuracy of order 4 cm. These sampling characteristics are sufficient to observe Rossby waves at periods longer than a few tens of days and wavelengths longer than a few hundred kilometers. Examples of this type of application are given and directions for future work are discussed.

Introduction

The focus of this paper is on propagating signals, especially Rossby waves, that are associated with topographic features. It is assumed that such propagating signals can have length scales as short as a few hundred kilometers and extend over thousands of kilometers. Similarly, it is assumed that the time scales can be as short as a few tens of days and that the signals can remain coherent over a year or more. Studying such signals from observations presents a formidable challenge, which can probably be met only through the use of remotely sensed variables.

The remote sensing variable of most interest to me is the sea surface height measured by satellite-borne altimeters. This interest stems from the fact that the sea surface height observations, when coupled with the hydrostatic approximation, give an estimation of the surface pressure field of the ocean. Thus, the satellite measurements yield observations of a dynamical variable that can be used more or less directly to diagnose the dynamics of the observed signals. This is in contrast to measurements of sea surface temperature, for example, which can change in response to thermodynamic forcing.

Three altimeters are relevant for the types of studies to be discussed in this paper. GEOSAT, which was flown by the U.S. Navy for geodetic reasons, returned 2 years of repeat cycle data that are particularly appropriate for oceanographic investigations. TOPEX/POSEIDON (T/P) was launched in 1992 as a joint project of the U.S. and France and is unique in that it was designed specifically for the purpose of obtaining high quality measurements of oceanographic variability. ERS-1, launched by the European Space Agency, also carries an altimeter, but these data are not discussed in this paper because at present the failure of the primary tracking system has prevented the determination of precise orbits, which are essential. An overview of results from GEOSAT can be obtained from JGR-Oceans special issues published in March and October of 1990. Also, Mitchum and Kilonsky (1995) have given a review of results from GEOSAT that focuses on the tropical portions of the oceans. T/P results also appear in a special issue of JGR-Oceans published in December 1994.

Mitchum (1994) described an extensive intercomparison of T/P sea surface heights (SSH) and in situ sea level observations from tide gauges. The basic result (Figure 1) is that for time scales longer than 10 days the two datasets agree to about 4 cm rms and have a correlation of 0.66. The rms differences can be significantly reduced, and the correlations increased, by smoothing the data to monthly means. In that paper a number of potential problems and biases were investigated, and one of these is of particular interest in the present context. Specifically, it was shown that for several sea level stations it was necessary to allow for signals propagating at the local Rossby wave speed (Gill, 1982) in order to obtain reasonable intercomparisons. This correction was necessary because the T/P ground track and the tide gauge location do not exactly coincide.

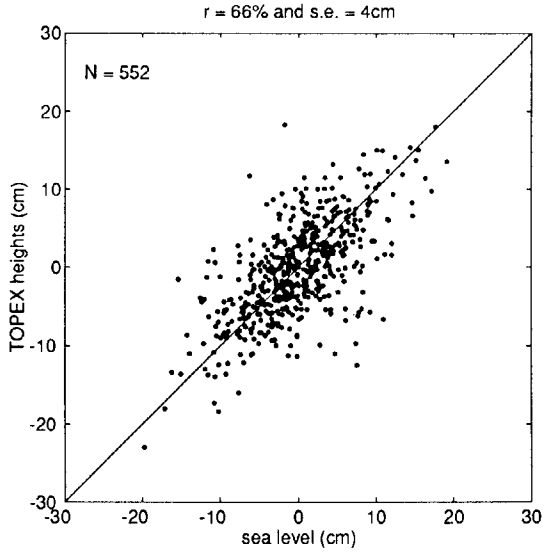

Figure 1. TOPEX sea surface height versus sea level data from tide gauges. Smoothing over 10-day intervals is performed before the data pairs are drawn. The scatter estimate is a robust estimate of the rms difference between the data pairs.

The station at Rarotonga in the South Pacific is a good example (Figure 2). In this case simply ignoring the zonal separation between the ground track and the tide gauge results in a correlation coefficient of -0.06. If, however, the time series are shifted by an amount corresponding to westward propagation at the Rossby wave speed, which was computed a priori rather than fit, the correlation increases to 0.62. Note also that the variance of the differences between the two time series has decreased by 55% as well. Looking at the series in more detail, it is clear that most of this improvement is due to a better match during the event that peaked around day 410, which had a duration of 100 days or so. It is difficult to say without more analysis, though, whether this signal is associated with a Rossby wave, an eddy, or something else.

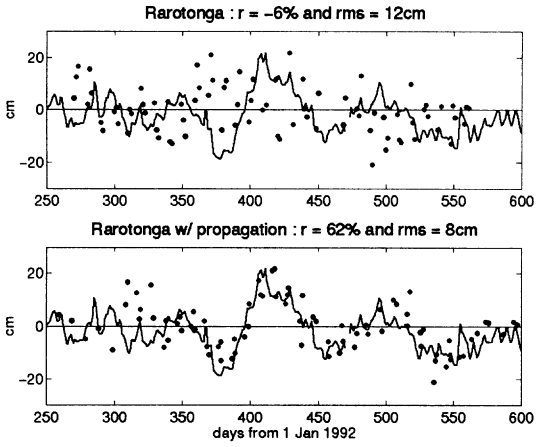

Figure 2. An example of a TOPEX to tide gauge comparison that is improved by allowing for Rossby wave propagation. The solid curve is sea level at Rarotonga and is the same in the upper and lower panels. The circles are the sea surface height values from TOPEX. In the upper panel the values are plotted at the time of observation, while in the lower panel the times are offset by an amount equal to the lag derived from the Rossby wave speed (computed to be 5.9 cm/s to the west) and the distance from the sea level station to the altimeter's ground track.

This paper describes two clear examples of Rossby wave signals observed from altimetric SSH and discusses some future directions for study. The first example is from an analysis of a Rossby wave signal observed at Wake Island in the western Pacific. This study used data from the GEOSAT mission and is described in more detail by Mitchum (1995a). The second example is from the T/P data and discusses a propagating signal found north of the Hawaiian Islands (see also Mitchum, 1995b).

Wake Island 90-day waves

Wake Island is located in western Pacific near 19°N and 166°E. Sea level from the tide gauge there shows an intermittent, but relatively large amplitude, oscillation at a period near 90 days (Figure 3). The data on this figure have been high-pass filtered, and the shaded regions mark time periods where the amplitude of the 90-day signal, as estimated by a complex demodulation, exceeds 8 cm. The years in this figure are aligned such that the leftmost 2 years on each line are ENSO events. It is apparent that the occurrence of the 90-day signals is modulated by ENSO, but the lag of 1-2 years is difficult to explain. In fact, these signals have been noted earlier (K. Wyrtki, personal communication), but the unusual phasing and the lack of other sea level records in the area made it impossible to diagnose the nature of these oscillations.

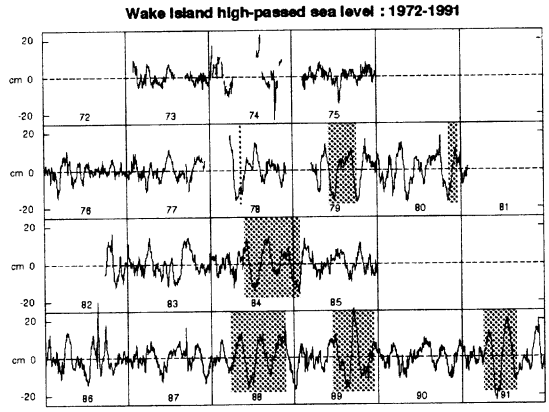

Figure 3. Daily sea level values from Wake Island after high-passing with a convolution-type filter having half-amplitude response at 200 d. Each line of the plot corresponds to the time series from the onset of an ENSO event to the beginning of the next event. Vertical lines are placed at 1 Jan of each year. Sea level units are cm. The shaded areas mark time periods where a complex demodulation analysis indicates that the amplitude of the 90-day oscillation is greater than 8 cm.

The timing of the GEOSAT mission, which produced good repeat cycle data from November 1986 to October 1988, was suitable for an analysis of the 90-day event observed at Wake Island in 1988. As discussed earlier for Rarotonga, it was apparent from simple correlation analyses that the signals were propagating westward at the local Rossby wave speed, and an analysis technique was devised to fit a zonal propagation speed to the GEOSAT space-time series. Briefly (see Mitchum, 1995a, for details), the calculation takes time series along a particular latitude and in an 8° longitude range and stacks them using phase lags computed from the longitude and an assumed propagation speed. The stacked series are then averaged, resulting in a single time series that emphasizes the propagating signals. Finally, the appropriate propagation speed is selected by requiring that the variance of this time series, as compared to a time series averaged without any lags, is

maximum. The results of this calculation for a particular point in space are estimates of the propagation speed, the variance ratio defined above, and a time series that emphasizes the propagating part of the signal.

This calculation was done with the GEOSAT data over much of the Pacific north of the equator, and the estimated zonal speeds were averaged zonally and plotted as a function of latitude (Figure 4). The f^{-2} behavior is consistent with Rossby waves and, since this was not imposed in any way by the fitting procedure, it serves as additional evidence that the propagating 90-day signal was in the form of a group of Rossby waves. One problem with this interpretation, however, is that the period of 90 days corresponds to a frequency that is theoretically too high to occur at this latitude. Based on an estimate of the Rossby radius obtained from several hydrographic profiles in this region (56 km), the mimimum period if the waves are at their turning latitude should be 120 days. It is possible to account for this difference by Doppler-shifting if it is assumed that the mean current is westward at 1-2 cm/s. Whether such a mean current exists is unknown, however, so it is only possible to say that the 90-day waves are close to their turning latitude.

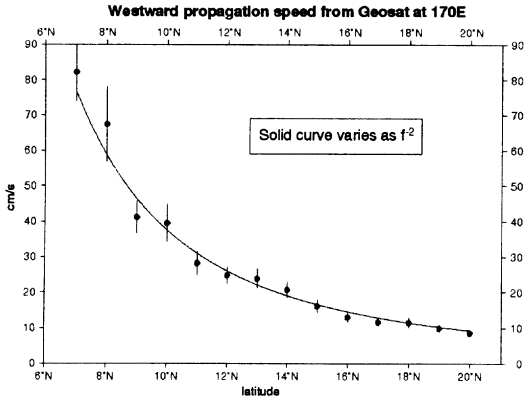

Figure 4. The solid circles represent the zonal average of the propagation speeds found from the procedure described in the text. At each latitude there are approximately 10 independent estimates of the propagation speed. The error bars represent 1 standard deviation about the zonal average. The solid curve shows the meridional variation expected for Rossby waves.

Although the GEOSAT data were very useful in characterizing the 90-day oscillations as Rossby waves in the vicinity of Wake Island, the real advantage of the SSH data is that the complete spatial coverage allows the tracking of the waves backward in time in order to locate the energy source. The fitting procedure used to estimate the wave speeds also returned a SSH dataset that emphasized the propagating signals. These data from the latitude of Wake Island (19°N) are plotted as a function of time and longitude in Figure 5. Similar plots were made at other latitudes (not shown) and these show that the signals observed at Wake Island are restricted to a narrow meridional band. Within this band, of which 19°N is typical, there is clear propagation to Wake Island from approximately 155°W, which corresponds to the longitude of the Big Island of Hawaii. Propagating signals are not significant east of Hawaii.

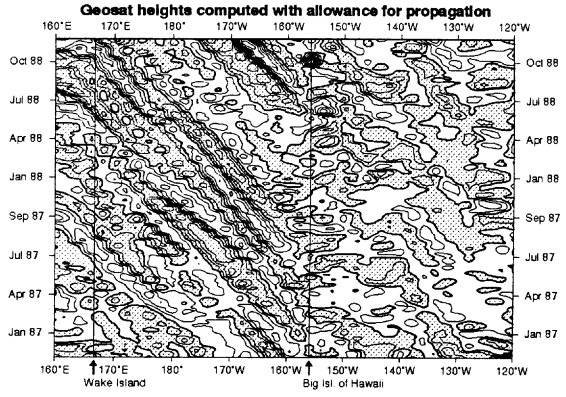

Figure 5. GEOSAT time series (computed with allowance for propagation) were formed between 160°E and 120°W and between 10° and 30°N. This figure shows a time-longitude cut along 19°N. This latitude falls close to both Wake Island and the Big Island of Hawaii. The slanting features in the left portion of the plot are propagating westward at about 7 cm/s. Negative sea surface heights are shaded and the contour interval is 3 cm.

The identification of the Big Island of Hawaii as the energy source for the Wake Island oscillations is also appealing because it helps to account for the phasing of the 90-day waves with ENSO events. The travel time from the Big Island to Wake Island is 1-2 years, which accounts for the observed lag if the energy source is active during the ENSO events themselves. There is thus no need to invoke unusual lags between the ENSO events and the excitation of the 90-day waves. It is still not clear, however, what process is responsible for the initial energy generation.

It is known (Patzert, 1969) that the area around the Big Island is rich with eddies. Different types of eddies are found in the area, however, and several possible generation mechanisms are likely. Regardless of how the eddies are generated, though, a likely scenario to account for the 90-day Rossby waves at Wake Island is that as the eddies propagate away from the topography, they decay into a train of Rossby waves, as described by Flierl (1977). It could be that the eddies are generated in response to flow past the Big Island, but the GEOSAT data are not adequate to examine this possibility. To examine this further, output from a numerical model (Hurlburt et al., 1992) was analyzed in the region of the Big Island. This analysis does in fact show that westward flow anomalies past the island give rise to anticyclonic eddies that separate from the topography and move westward. The model does not, however, decay these

eddies into a Rossby wave train, or reproduce the sea level time series at Wake Island. So, for the present, this scenario remains speculative. Also, since the agreement between model and data was not very good, it was not considered useful to diagnose the eddy generation mechanism in detail. In the paper referred to earlier (Mitchum, 1995a), however, several possibilities are discussed in more detail.

Waves north of the Hawaiian Ridge

The second example of Rossby wave signals from altimetry is from the area north of the Hawaiian islands and comes from the T/P dataset, which is significantly more accurate than the GEOSAT data. This study was motivated by observations from the Hawaiian Ocean Time-series (HOT) site (Karl and Lukas, 1995). Briefly, the HOT program involves the collection of a variety of physical, geochemical, and biological measurements at a single deep water location approximately 100 km north of the Hawaiian Ridge. The target is to make monthly measurements, and the program has been collecting data for over 5 years. A more complete description of the specific results given below can be found in Mitchum (1995b).

During part of the HOT program, time series of dynamic height were estimated from moored inverted echo sounders, which were calibrated against CTD data to give dynamic height differences from 0-1000 db. These measurements revealed a prominent, but intermittent, 130-day signal (Chiswell, 1995), and it should be noted that similar signals have also been observed in GEOSAT and AVHRR measurements (van Woert and Price, 1993). It was natural to ask whether the T/P data could provide a larger scale diagnosis of the nature of these oscillations, and the first question is simply whether the T/P SSH data reproduce these signals at the HOT site. This was addressed by intercomparing the T/P SSH and the dynamic height time series from the HOT site (Figure 6). Although the period of overlap in the two measurements is only about 6 months long, it is clear that the T/P SSH captures the oscillations.

In order to extend these results to a larger spatial area, an extended empirical orthogonal function (EEOF) analysis was carried out. This analysis is designed to capture propagating features, and the 130-day signals were emphasized by high-pass filtering the SSH time series prior to the analysis. The main result from the EEOF analysis is that the 130-day oscillation is very well described by a simple 130-day harmonic with a spatially dependent amplitude and phase functions that slowly vary in time. Since this alternate description is simpler to present and to interpret, the remainder of this discussion will focus on the modulations of the amplitude and phase of this 130-day sinusoid.

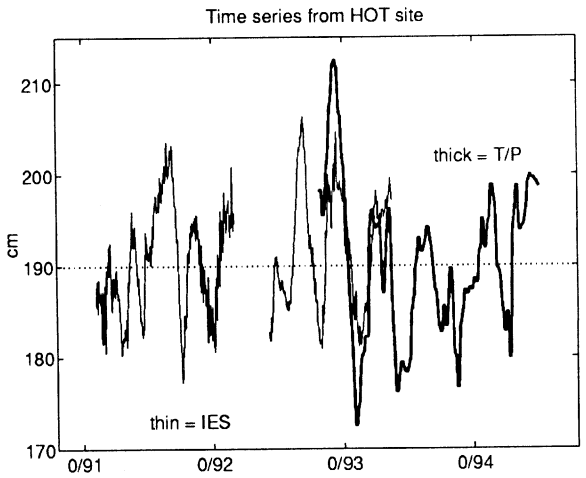

Figure 6. Combined height series from IES data and T/P data. The T/P data are from the crossover point lying immediately northeast of the HOT site. The T/P data are interpolated to a regular grid via an objective interpolation and then joined to the IES height series. The T/P series is lagged by 20 days in order to align the high frequency events. This lag was chosen to give the best fit between the two series, but it is also consistent with the propagation characteristics described in the text. The times are given as Julian day/Year.

The amplitude function is shown in Figure 7. The amplitude of the 130-day signal is initially large near 158°W and just north of the Hawaiian Ridge. The amplitude subsequently evolves away to the north and west, reaching 165°W after 1 year. If this amplitude evolution is interpreted in terms of Rossby wave theory, then this implies that the group velocity is to the northwest. If this is correct, then the phase velocity should be to the southwest.

The phase of the oscillation is represented somewhat differently (Figure 8). In this case it was found that the basic pattern of phase did not change appreciably in time, and so the phase of the mean harmonic at each point in space is shown. Note, however, that the phase is only interpretable when the amplitude is significant, so the phases at any particular location on this figure should only be interpreted as relevant during a temporal subset when the amplitude function (Figure 7) is large at that location. During the earlier times when the signal is near 158°W, the phase propagation is indeed to the southwest in qualitative agreement with theory. Calculation of the actual phase gradient do in fact reproduce the expected phase speed as well.

At the later times, as the area with large amplitudes moves north and west, the phase lines align north-south, indicating westward phase propagation. There is also a suggestion near 165°W that the meridional component of the phase velocity has reversed. This is especially interesting because it could indicate that the Rossby wave packet has reached its turning latitude, and to my

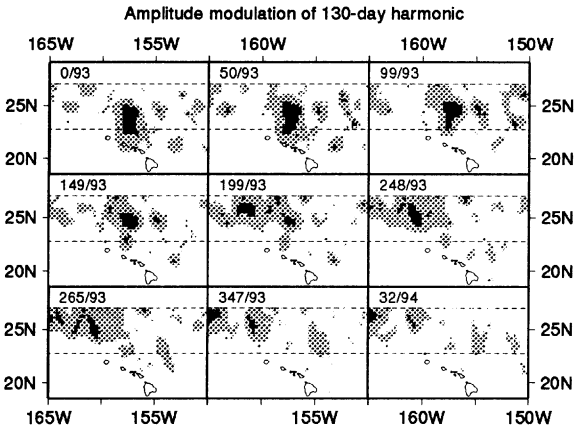

Figure 7. Amplitude of the 130-day harmonic as a function of space and time. The amplitude of a 130-day harmonic is computed along all of the T/P ground tracks north of the ridge and south of 27°N in an overlapping sequence of 200-day intervals. The results are interpolated to a regular spatial grid before drawing the images. Each successive panel in the figure is separated by just under 50 days, and the time associated with each map is given in the upper left hand corner of each panel as Julian day/Year. The light gray shows regions where the amplitude exceeds 5 cm; the dark gray is where it is greater than 10 cm. The broken lines drawn at the latitude of the HOT site and at 27°N are shown to aid the evaluation of meridional propagation.

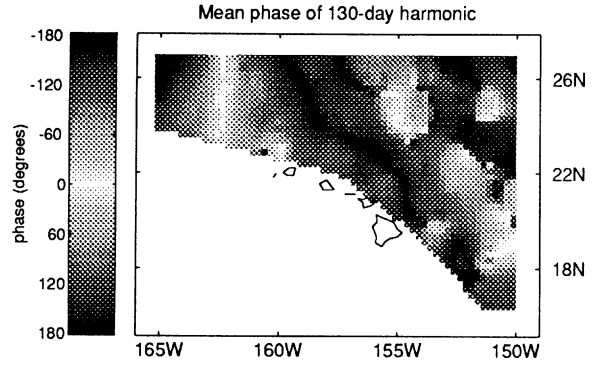

Figure 8. Spatial description of the phase of the 130-day harmonic. To form the phases shown in this figure the sine and cosine coefficients from the harmonic fits in overlapping 200-day intervals are averaged, and the phase is computed from the resulting mean harmonic. This averaging was done only after it was noted that the phase maps from the individual 200-day intervals were similar in pattern in the regions with significant amplitudes. The gray scale is cyclical, with phases of 0° in white and phases of 180° and -180° in black.

knowledge this phenomenon has not been previously observed for Rossby waves. As in the case of the Wake Island wave, the observed period places the wave close to the turning latitude. It is difficult to say at this point whether this interpretation is correct, and this problem will be revisited when longer time series are available.

Work in progress

The use of the altimetric SSH data in the examples given in the previous sections has been motivated by first finding strong oscillatory signals in other in situ time series of sea level or dynamic height. Basically, the better temporal coverage and accuracy of the in situ data makes it easier to identify interesting signals, after which the altimetric data are examined in order to place these point time series in a spatial context. Given the success of the altimetric SSH, especially for T/P, in reproducing the observed signals, it seems reasonable to search for propagating signals using the altimetric SSH alone. At present I am not satisfied with the techniques tried thus far to identify such signals, such as the method described for the Wake Island waves. This method does, however, allow a simple beginning along this new line of investigation, and this calculation was therefore extended to cover the Pacific between 10° and 50° in both hemispheres.

The zonally averaged speed estimates from this calculation, which are analogous to those shown in Figure 5, are shown in Figure 9. The speed estimates match the theory well, indicating that Rossby waves are ubiquitous and relatively easy to identify from the SSH data. It is interesting to note the closer correspondence with theory in the southern hemisphere. If the deviations in the fitted speeds are indeed due to Doppler-shifting, then this may be a consequence of the fact that the subtropical gyre in the southern hemisphere is relatively weak as compared to the northern gyre.

The calculation also results in an estimate of the variance ratio of the propagating signals relative to the stationary ones. When this ratio is large, it indicates that the propagating signals are dominant and that the calculation is sensible. In fact, the speed estimates shown

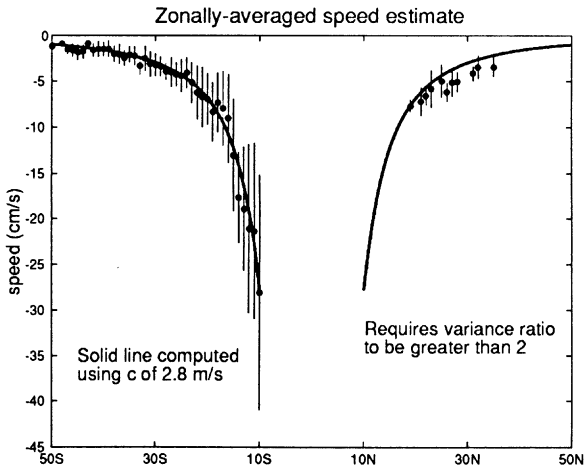

Figure 9. As in Figure 4, but from the larger scale calculation using the T/P sea surface height data.

on Figure 9 only use grid points where the variance ratio exceeds 2. A map of points where this occurs (Figure 10) shows crudely where the propagating signals are largest. Note the tendency for the points to lie in the western half of the basin in both hemispheres, again indicating that the

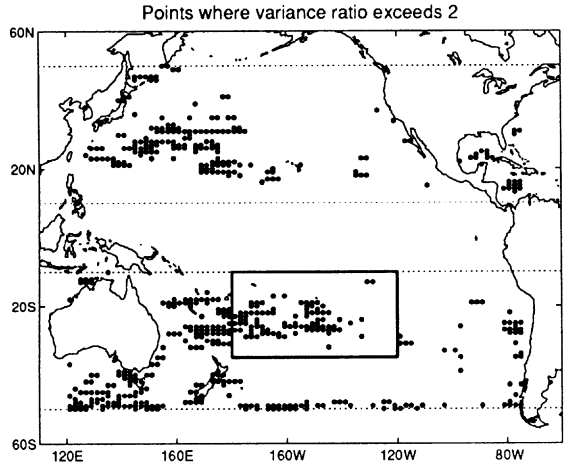

Figure 10. The variance ratio (described in the text) is large when propagating signals dominate the sea surface height time series. Solid circles are placed at grid points where the variance ratio is larger than 2. The spatial grid is 1° latitude by 2° longitude.

calculation is indeed capturing Rossby wave activity. Note also the relatively large number of points in the southern hemisphere. Whether this indicates larger propagating signals, smaller background (stationary) signals, or problems with the analysis is not known at present.

An enlargement of the area in the southern hemisphere bounded by the box is shown in Figure 11. This region was enlarged because it marks a zonal transition from relatively weak propagating signals to strong ones, in analogy to the behavior westward of the Hawaiian Ridge. The analogy appears to be useful, in that the variability

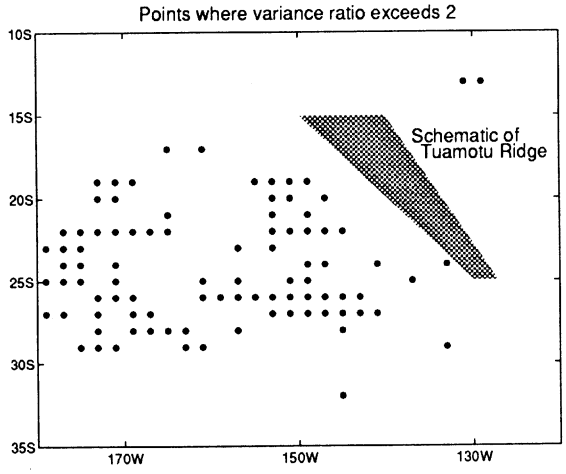

Figure 11. Enlargement of Figure 10 to show the effect of the Tuamotu Ridge.

does occur to the west of a topographic feature, namely the Tuamotu Ridge. Future studies of the wave and eddy signals west of the Hawaiian Ridge will therefore also consider this southern hemisphere analog.

Although the calculation used here to identify propagating signals has worked reasonably well in areas where the propagating signals are relatively large and coherent, it will certainly not work with more subtle signals. Better techniques need to be developed and a number of possibilities are being investigated. Even with this limited tool, however, it is clear that signals propagating at the local Rossby wave speed are common, and often appear to be linked with topographic features.

Finally, recall that both of the prominent signals that I have described appear at frequencies that suggest these waves are found very near their turning latitudes. Although this might be coincidental, it is very intriguing. According to theory, this latitude should trap energy at that period, and verifying this observation in a more general way would be a novel application of the altimetric SSH data.

Acknowledgments. This work was supported by NASA through the Jet Propulsion Laboratory as part of the TOPEX Altimeter Research in Ocean Circulation Mission.

References

Chiswell, S., 1995: Intraseasonal oscillations at Station ALOHA, north of Oahu, Hawaii. *Deep-Sea Res.*, in press.

Flierl, G., 1977: The application of linear quasigeostrophic dynamics to Gulf Stream Rings, *J. Phys. Oceanogr.*, 7, 365-379.

Gill, A., 1982: *Atmosphere-Ocean Dynamics*. Academic Press, Orlando, Florida, 662 pp.

Hurlburt, H., A. Wallcraft, Z. Sirkes, and E. Metzger, 1992: Modeling of the global and Pacific oceans: On the path to eddy-resolving ocean prediction, *Oceanography*, 5, 9-18.

Karl, D. and R. Lukas, 1995: The Hawaii Ocean Time-series (HOT) program: Background, rational and field implementation. *Deep-Sea Res.*, in press.

Mitchum, G., 1994: Comparison of TOPEX sea surface heights and tide gauge sea levels. *J. Geophys. Res.*, 99, 24,541-24,554.

Mitchum, G., 1995a: The source of 90-day oscillations at Wake Island. *J. Geophys. Res.*, 100, 2459-2476.

Mitchum, G., 1995b: On using satellite altimetric heights to provide a spatial context for the Hawaii Ocean Timeseries measurements, *Deep-Sea Res.*, in press.

Mitchum, G., and B. Kilonsky, 1995: Observations of tropical sea level variability from altimeters, To appear in *Oceanographic Application of Remote Sensing*, M. Ikeda and F. Dobson (eds.), CRC Press, Boca Raton, FL.

Patzert, W., 1969: *Eddies in Hawaiian waters*. Technical Report HIG-69-8, Hawaii Institute of Geophysics, University of Hawaii, Honolulu, 51 pp.

van Woert, M. and J. Price, 1993: GEOSAT and Advanced Very High Resolution Radiometer observations of oceanic planetary waves adjacent to the Hawaiian Islands. *J. Geophys. Res.*, 98, 14,619-14,632.